The Journal of Experimental Biology 205, 2005–2016 (2002)
Printed in Great Britain © The Company of Biologists Limited 2002
JEB4203E

S- and C-start escape responses of the muskellunge (*Esox masquinongy*) require alternative neuromotor mechanisms

Melina E. Hale

Department of Organismal Biology and Anatomy, University of Chicago, 1027 East 57th Street, Chicago, IL 60637, USA

e-mail: mhale@uchicago.edu

Accepted 1 May 2002

Summary

The startle response is a model system for examining the neural basis of behavior because of its relatively simple neural circuit organization and kinematic pattern. In fishes, the two primary types of startle behavior differ in their initial movements. In the C-start type of startle, the fish bends into a C shape, while the S-start involves an S-shaped body bend. Although considerable research has focused on determining how the C-start is generated neurally, S-start neurobiology has not been examined. I quantify the kinematics and electromyographic patterns of the initial movements of the C-start and S-start behaviors of the muskellunge (*Esox masquinongy*) to test three hypotheses for how the S-start is generated. (i) The S-start is generated by the same motor neural circuit as the C-start, but passive bending of the tail causes the body to take on an S shape. (ii) The S-start is generated by the same motor neural circuit as undulatory swimming. (iii) The S-start is generated by an independent neural mechanism from that used either in the C-start or in undulatory swimming. Results from kinematics and muscle activity patterns support the third hypothesis. In the muskellunge, the S-start is a high-performance startle behavior with peak angular velocity and peak angular acceleration of its initial bending comparable with those of the C-start and higher than would be expected for undulatory swimming. The S-start motor pattern, however, is distinct from the C-start motor pattern in having simultaneous muscle activity anteriorly on one side of the body and posteriorly on the opposite side. In contrast, the C-start is characterized by simultaneous unilateral muscle activity along the full length of the body. Alternative models are proposed for S-start neural circuit organization involving reticulospinal and local control of muscle activity.

Key words: swimming, fast-start, neural circuit, startle, muskellunge, *Esox masquinongy*, electromyography, C-start, S-start.

Introduction

Fast-start escape responses are high-acceleration startle behaviors commonly used by fishes and aquatic amphibians to avoid predators. Two types of fast-start have been identified kinematically, the S-start and the more common C-start. During the C-start, the fish turns away from an offending stimulus by bending into a C shape in its initial, or stage 1 (Weihs, 1973), movement prior to forward propulsion. This bend is frequently followed by large-amplitude axial motions characteristic of burst swimming. The net trajectory of center of mass motion during the C-start can occur in any direction relative to the fish's initial orientation (Domenici and Blake, 1991; Foreman and Eaton, 1993). During the S-start, the fish forms an S shape with its body rather than a C shape. The S-bend is followed by an L-shaped bend and then rapid undulatory swimming. In addition to its function as an escape response, S-start behavior is also used during prey strikes (e.g. Webb and Skadsen, 1980; Rand and Lauder, 1981; Harper and Blake, 1991; Frith and Blake, 1995; Johnston et al., 1995) and has more frequently been studied in this role. In both tail-elicited escape behavior and strike S-starts, the fish moves forward through the water either away from its predator or towards its prey.

The morphology and physiology of the neural circuit that drives the C-bend have been studied in depth (e.g. Furukawa and Furshpan, 1963; Hackett and Faber, 1983; Fetcho and Faber, 1988; Faber et al., 1989; Fetcho, 1991). The C-start is initiated by the Mauthner cells, a pair of large commissural reticulospinal interneurons. The Mauthner cell somata are located in the hindbrain, one on each side of the body. The axon of each Mauthner cell crosses the longitudinal midline of the body and extends the full length of the spinal cord on the opposite side of the body from its soma. Commissural hindbrain interneurons reciprocally inhibit the Mauthner cells, preventing them from firing together (Furukawa and Furshpan, 1963; Hackett and Faber, 1983) and sending conflicting signals to spinal cord circuits. Combinations of pairwise intracellular physiological recordings with corresponding cell staining for morphology have provided a well-supported model for the

spinal cord circuit of the C-start behavior (Fetcho and Faber, 1988; Fetcho, 1991). Both directly and indirectly through ipsilateral excitatory interneurons (Fetcho and Faber, 1988), the Mauthner cell excites motoneurons on one side of the body. Through commissural inhibitory interneurons, it inhibits motoneuron activity on the opposite side (Fetcho, 1990). The activation of this circuit causes the rapid and nearly simultaneous contraction of the axial muscle of the fish that results in the C-bend.

While the C-start has been the focus of much behavioral and neural research, few studies have examined S-start escape kinematics (Webb, 1976; Harper and Blake, 1990; Spierts and Van Leeuwen, 1999) and none have examined the neuromuscular physiology of the response. An important question that has not been addressed is, what is the neural mechanism that produces the S-start? One hypothesis is that the S-start may involve the same neural mechanisms as the C-start, but that the reverse bend at the tail results from passive fluid loading (Domenici and Blake, 1997). In the C-start of the sunfish *Lepomis macrochirus*, the tail bends in the opposite direction to the anterior body (Jayne and Lauder, 1993, 1996) so that the fish does not perform a true C-shaped C-start. Jayne and Lauder (1996) attributed the backward bend of the tail to the resistance of the water on the caudal fin. It has been suggested that the same effect could cause the S-shaped body form of the S-start from a C-start motor pattern (Domenici and Blake, 1997).

Two alternative hypotheses for how the S-start is generated neurally have not been discussed in the literature. First, the S shape may not involve a rapid startle circuit but instead result from a wave of muscle activity along the body similar to that typically associated with a rhythmic swimming motor pattern. In this case, the S-start would be equivalent to the initiation of a burst swimming event, a slower response than a C-start. There is some evidence for this hypothesis from performance data comparing C-start and S-start escape responses. Mean and mean maximum accelerations are significantly higher in C-starts than in S-starts in northern pike (*Esox lucius*) (Harper and Blake, 1990) and in carp (*Cyprinus carpio*) (Spierts and Van Leeuwen, 1999), although this was not the case in the rainbow trout (*Oncorhynchus mykiss*) (Harper and Blake, 1990).

Second, the S-start, like the C-start, may be a high-performance startle behavior, but may be generated with a neural circuit different from that for either the C-start or swimming. Instead of generating nearly simultaneous muscle contraction on one side of the body and inhibiting contraction on the other, this circuit would generate muscle activity rostrally on one side and caudally on the other side to form the S-shaped bend. Regional activity on both sides of the body cannot be explained by the current model of Mauthner-cell-initiated C-start behavior, implying that a fundamentally different circuit would have to mediate the S-start behavior.

To discriminate among possible explanations for how the S-start behavioral pattern is generated, kinematic patterns and electromyographic (EMG) activity were recorded simultaneously for escape responses of the muskellunge (*Esox masquinongy*). I focused on stage 1 of the fast-start because it is the stage 1 data that address the startle mechanisms discussed above. If the performance (assessed by angular velocity and angular acceleration) and muscle activity patterns of the S-start are the same as those for the C-start, then the first explanation, that passive external loading causes the S-shaped body bend, would be supported. If the performance of the S-start is significantly lower than that of the C-start and the myomeres are active in a rostrocaudal wave of activity along the body, it would suggest that the S-start is more similar to steady swimming than to the C-start, in which myomeres are active nearly simultaneous along the length of the body. If the performance of the S-start is not significantly poorer than that of the C-start but there is regional muscle activity on both sides of the body simultaneously, then the third possible explanation, that the S-start is generated by a different neural circuit to the C-start, would be supported.

Materials and methods

Study animals

Muskellunge (*Esox masquinongy* Mitchill 1824) were provided by the Jake Wolf Fish Hatchery, Illinois Department of Natural Resources, USA. Five fish ranging in length from 318 to 351 mm (333±14 mm, mean ± S.D.) were examined. At the hatchery, muskellunge were maintained in a large lake as breeding stock. The fish were transported to the Field Museum of Natural History, where they were held in tanks at 20 °C. Fish were kept in the laboratory for 3 weeks while experiments were being conducted. During this time, they were fed minnows on alternate days. Fish were not fed for 24 h prior to an experiment.

The muskellunge was chosen because it readily performs S-start and C-start behaviors. In addition, most previous studies on S-start behavior have looked at congenerics (e.g. Webb, 1976; Webb and Skadsen, 1980; Rand and Lauder, 1981; Harper and Blake, 1990; Webb et al., 1992; Frith and Blake, 1995). The close relationship and similar morphology of these species simplify cross-study comparisons.

Kinematics

Fast-start kinematic patterns were recorded in the study fish before electrodes were implanted for electromyograms as controls for the electromyographic (EMG) data. Experiments were repeated after surgery while simultaneously recording electromyograms. S- and C-start escape responses were elicited by touching or pinching the tail for S-start responses with metal forceps or with the hands and by touching the head with a dowel for C-start responses. Kinematic patterns were recorded from a ventral view. Fish were centered in the tank and were holding station in midwater when the stimulus was applied.

Fast-starts were recorded at 500 frames s^{-1} with a Redlake PCI-1000S digital high-speed video camera. Images were viewed and digitized with NIH Image 1.60. Analysis focused

Table 1. *Positions of the center of mass and electrodes relative to total body length*

Landmark	Position (% *BL*)	Range (% *BL*)
Center of mass	42.9±0.3	48.4–49.6
Electrodes 1 and 4	34.8±0.6	32.8–36.4
Electrodes 2 and 5	49.8±0.6	48.1–51.7
Electrodes 3 and 6	69.2±0.3	69.2–70.1

Position values are means ± S.E.M., *N*=5.

Total body lengths (*BL*) ranged from 318 to 351 mm (333±14 mm, mean ± S.D., *N*=5).

on the first stage of the fast-start in which the fish forms the C- or S-shaped movement. Data for the duration and angle of movement were taken directly from the video recordings. The angle through which the head turned during the fast-start stages was measured with NIH Image 1.60. Other kinematic parameters were analyzed from digitized images. I digitized the outline of the fish of every other image so that the effective frame rate for these variables was 250 Hz. The points were digitized from the ventral view of the fish along the margins of the body (not including the fins). Points along the midline representing intervals of 5 % of standard length *SL*, at the positions of the electrodes and at the center of mass (Table 1), were determined, and bending at these points was calculated from the digitized outline points using a midline analysis program (Jayne and Lauder, 1995). Angular velocity and acceleration were calculated with QuickSAND, a numerical differentiation program written by J. A. Walker (Walker, 1998). I focus on angular velocity and acceleration rather than linear acceleration of the center of mass (e.g. Harper and Blake, 1990; Spierts and Van Leeuwen, 1999) because of this study's focus on the initial bending movements that are generated by known startle neural circuits including the Mauthner cells. These early movements are primarily rotational, involving little or no forward acceleration, as can be seen in plots of accelerometer data (Harper and Blake, 1990).

Electromyography

Electromyograms were recorded with fine-wire electrodes implanted in epaxial muscle. Electrodes were made from 0.05 mm diameter double-stranded, insulated, stainless-steel wire. The ends of the wire were split, separating the two strands. Insulation was removed from the tip of each strand (approximately 2 mm), and the strands were bent back to separate the stripped areas and to help hold the electrodes in position in the muscle. Electrodes were threaded into 25 gauge needles that could be easily inserted through the skin and into the myomeres.

Prior to surgery, the experimental fish was anesthetized with 3-aminobenzoic acid ethyl ester (MS222) in water. Once sedated, six electrodes, three on each side of the body, were implanted into large cones of white muscle fibers in the epaxial region of the myomere at approximately 1 cm depth. Fig. 1 and Table 1 show the longitudinal positions of the electrodes and the variation in the exact placement of the electrodes among the fish. The electrode positions were chosen on the basis of control S-start kinematics in order to record muscle activity in both trunk and tail bends. After experiments, the study animals were killed with an overdose of MS222. Measurements of total and standard length, and the longitudinal positions of the center of mass and electrodes, were recorded. The longitudinal position of the center of mass was determined by laying the fish lengthwise on a balance (a lever supported in the middle) so that rostral and caudal body regions maintained equilibrium.

electromyograms were recorded on a TEAC eight-channel DAT tape recorder; 5000 points s^{-1} were collected for each of the six electrode channels. An additional channel collected the square-wave signal that was simultaneously recorded onto the kinematic sequences so that electromyograms and kinematic patterns could be synchronized for analysis. The relative timing of electromyographic (EMG) activity to movement as well as the EMG amplitudes, durations and were analyzed with LabView Virtual Instrument Software (National Instrument Corporation, Austin, Texas) using custom-designed virtual instruments and an NB-MIO-16 analog-to-digital converter.

Statistical analyses

Three trials of each fast-start type were analyzed for each of the five fish. Trials were analyzed from fish turning to the right and to the left because there was no difference in the response between the sides. To combine trials of right and left turns, the data were standardized to the direction of head movement. Multivariate analysis of variance (MANOVA) was used as a global test for differences between the C-start and S-start and among the individual fish for kinematic and EMG data sets with JMP statistical software (JMP 3.1.6, SAS Institute). In addition, I used analysis of variance (ANOVA) with repeated measures in the program SuperANOVA (Abacus Concepts, Inc.) for the Macintosh to test for specific differences in kinematics and EMG variables. Sequential Bonferroni tests (Holm, 1979; Rice, 1989) were applied to kinematic and EMG data to adjust significance levels for multiple tests. When a *P*-value was less than 0.05 but did not meet the Bonferroni-adjusted significance level (α=0.05), it is noted in the text.

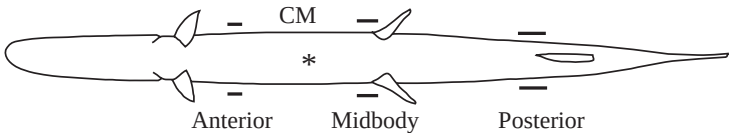

Fig. 1. Center of mass (CM; *) and electrode positions for fast-starts of the muskellunge (*Esox masquinongy*). Horizontal lines indicate the approximate longitudinal variation in electrode positions among the study animals quantified in Table 1.

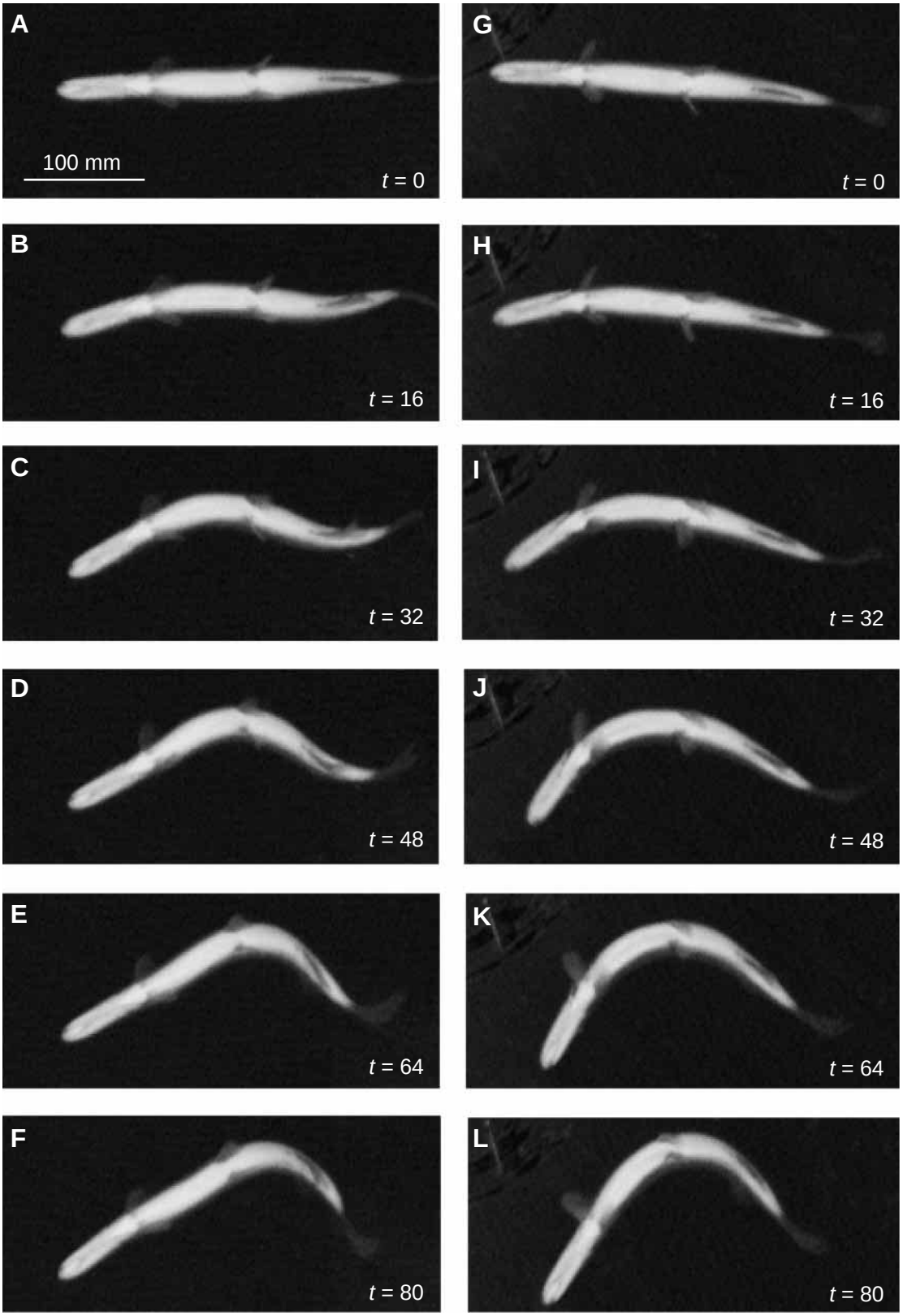

Fig. 2. The initial movements of an S-start and a shallow C-start of the muskellunge (*Esox masquinongy*). (A–F) S-start behavior of the muskellunge. The fish bends into an S shape early in the behavior, 16–32 ms after initiation of movement (B,C) followed by the return of the tail in the opposite direction to form an L-shaped bend by 64 ms. (G–L) A shallow C-start. A comparison of S-start images B and C with C-start images H and I demonstrates the difference in caudal bending between these two response types. Time (*t*) is shown in milliseconds. Scale bar, 100 mm.

Results

Kinematics

S- and C-starts of the muskellunge have distinct kinematics that are consistent within each fast-start type. MANOVA examining the effects of fast-start type, individual and the interaction between them demonstrates a significant difference in the whole-model effect (Wilks' lambda, F=2.64, P<0.002), with a significant effect of fast-start type (Wilks' lambda, F=20.47, P<0.0001) and no effect of individual (Wilks' lambda, F=1.33, P=0.23) or interaction between fast-start type and individual (F=1.34, P=0.23). Fig. 2A–F shows bending during the S-start behavior prior to forward propulsion, which has two kinematic phases. First, the fish bent its head and trunk to one side of the body and its tail to the opposite side so that an S shape was formed (Fig. 2B). Following the S-bend, the tail bent back in the same direction as the rest of the body to form an L shape (Fig. 2E) similar to the C-shaped body bend during stage 1 of the C-start (Fig. 2K). This second bend of the tail occurred prior to waves of bending along the body and forward propulsion equivalent to stage 2 and stage 3 and subsequent swimming tail strokes (Weihs, 1973) of the C-start. Stage 1 of the C-start involved a single bend to one side of the body. In Fig. 2G–L and Fig. 3, two C-starts are shown. Fig. 2G–L depicts images of a C-start with comparable bending to the representative S-start (Fig. 2A–F) to illustrate the difference in caudal bending during S-starts and C-starts that involve a similar degree of head movement in stage 1. In Fig. 3A–F, a C-start with a higher degree of bending and greater

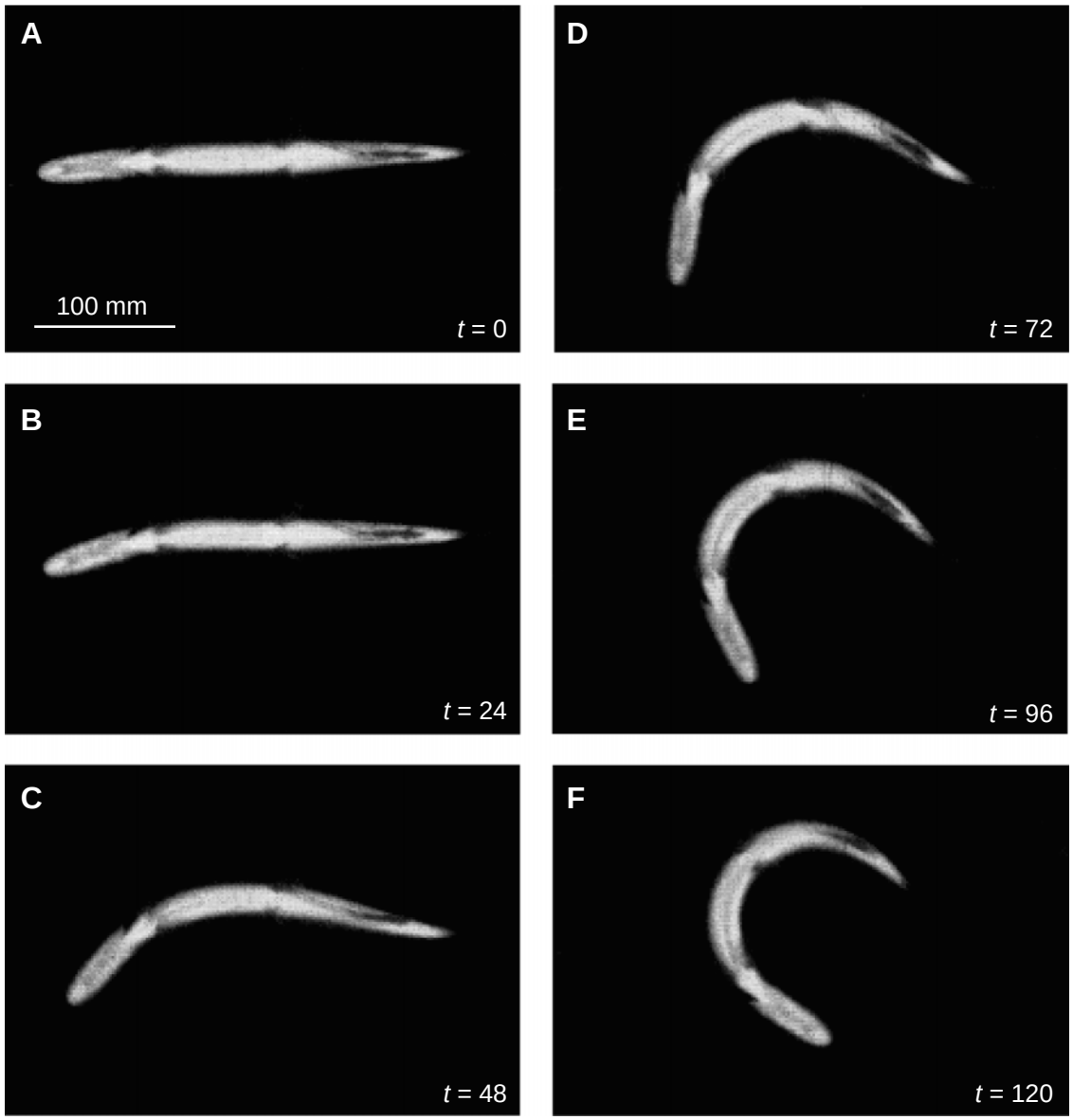

Fig. 3. A larger-amplitude C-start of the muskellunge (*Esox masquinongy*). (A–F) A C-start with greater and more typical initial bending than that shown in Fig. 2. As with the shallower C-start (Fig. 2G–L), this C-start with greater curvature does not show the bending contralateral to the rostral bend evident during the S-start. Time (t) is shown in milliseconds. Scale bar, 100 mm.

turn angle is shown. This is a more typical C-start movement pattern for the muskellunge. During both small- and large-angled C-starts of the muskellunge, tail bending in the opposite direction to the major rostral bend is limited to the caudal fin.

Body bending, the angle of head movement and the duration of movements were compared between S-starts and C-starts. Body bending was measured at the electrode positions and at the center of mass (Table 2). During the S-bend, the angle of bending of the tail, measured at the third electrode position, was significantly different from bending at the other positions (P<0.0001). Although the magnitude of bending was similar among the positions (average bending ranged from 3 to 5 °), the tail at electrode position 3 bent to the opposite side of the body from the more rostral anterior and midbody electrode positions and from the center of mass. The L-bend that followed the S-bend involved significantly greater curvature at the midbody electrode position (on average, 8 °) than at the other three positions (all less than 4 °) (P<0.005; Table 2). For the C-start, bending along the full length of the body was to the same side, the side opposite the stimulus, with average bending ranging from 3.8 to 8.2 ° (Table 2).

There were significant differences in the bending patterns of the S-start and the C-start behaviors. Comparing the L-bend of the S-start and the C-bend of the C-start, bending at the center of mass and at the caudal electrode position differed, being greater for the C-bend than for the L-bend. Although P<0.05 for these variables, when a sequential Bonferroni test was applied to the kinematic data (Holm, 1979; Rice, 1989), the bending at the center of mass and caudal electrode position did not meet the adjusted significance level of slightly greater than 0.01. While the L-bend involved a high degree of local bending in the midbody region with significantly less bending around it (P<0.005), the C-bend involved a higher degree of bending along the full length of the body. Comparing the S-bend with the C-bend, the major difference was in caudal bending, which was of the same magnitude but to the opposite side of the body. I also compared the S-bend with the C-bend at the same point in time, 16 ms (close to the time of the maximum S-bend) after startle initiation, to determine whether the C-start involved an S-shaped bend prior to taking on its C-shaped bend at the end of stage 1. The difference in caudal bending was significant (P<0.005). Even at the beginning of the C-start, the body took on a C shape, with the tail bending in the same direction as the major body bend.

The durations of stage 1, from initiation through the L-bend of the S-start and the C-bend of the C-start, were not significantly different between fast-start types, with means of 81 and 108 ms, respectively, for the S-start and C-start. The duration of the S-bend, with a mean of 35 ms, was significantly shorter than that of either the L-bend (from initiation) of the S-start or the C-bend of the C-start (P<0.0001; Table 2). The C-starts of muskellunges recorded by Webb et al. (1992) were considerably shorter in duration than the C-starts I recorded. However, these differences may be due to the larger size of the fish used in the present experiments or to differences in stimulus methods, tactile stimuli in the present study compared with electric shocks in the previous work (Webb et al., 1992). The angle of head movement was significantly lower for the S-start than for the C-start (P<0.0001), with the mean angle of head movement through the L-bend being 43.9 ° compared with 98.1 ° for the C-bend (Table 2). Much of the angular movement during the S-start occurred during the initial S-bend, on average, 27.7 °.

Angular head velocity and angular head acceleration were used to compare performance between the S- and C-starts. There was no significant difference between either maximum velocity (P=0.0763) or maximum acceleration (P=0.0861; Table 2), indicating that the S-start is a high-performance startle behavior comparable with the C-start. Fig. 4 shows plots of head angle, angular velocity and angular acceleration through the response. Visual comparison of these plots suggested that the differences between C- and S-starts were not in the peak velocity or acceleration but in how long maximum angular velocity was maintained during the movement. Fig. 4 illustrates how head angle changes through typical S-start and C-start behaviors. During the C-start, the head angle increased

Table 2. *Kinematic variables of S-start and C-start behaviors*

	S-start		C-start
	S-bend	L-bend	C-bend
Bending at the center of mass (degrees)	3.94±0.32	3.75±0.74	6.01±0.41
Bending at E1/E4 (degrees)	3.12±0.48	3.47±1.16	6.89±1.15
Bending at E2/E5 (degrees)	4.69±0.72	8.02±0.98	8.23±0.99
Bending at E3/E6 (degrees)	–3.36±0.34	0.34±0.90	3.84±0.72
Duration from initiation (ms)	35±1	81±5	108±11
Head angle from initiation (degrees)	27.7±2.7	43.9±6.4	98.1±11.2
Maximum angular velocity (degrees ms^{-1})	1.99±0.19	–	2.43±0.15
Maximum angular acceleration (degrees ms^{-2})	0.22±0.03	–	0.15±0.02

For the S-start, kinematic patterns were measured at the end of S- and L-bends and for the C-start at the end of the C-bend.
All measurements are means ± S.E.M.; N=15 trials per fast-start type; three trials for each of five individuals.
There was no peak in angular velocity or angular acceleration during the L-bend of the S-start.
E1–E6, electrodes 1–6.

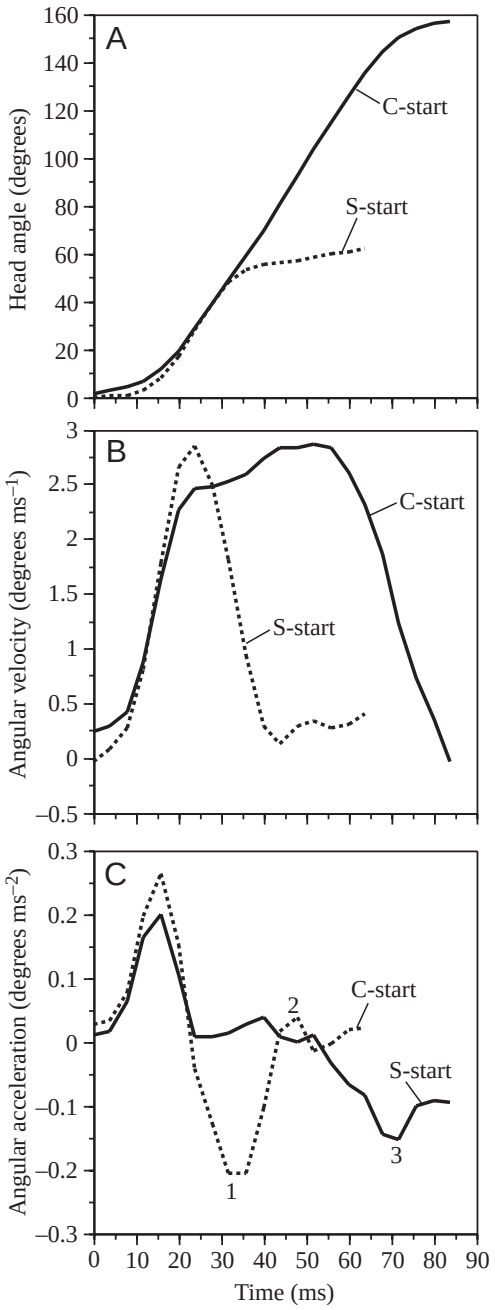

Fig. 4. Profiles of head angle (A), angular velocity (B) and angular acceleration (C) through S-start and C-start behaviors. Numbers on the angular acceleration plot indicate the end of the S-bend (1), the L-bend (2) and the C-bend (3).

over a much longer period, resulting in the significantly greater head angle. This increase in head angle through the C-start occurred at peak angular velocity. Velocity plateaued near its maximum value during the C-start and remained elevated much longer than it did in the S-start. This was also reflected in the plateau at near zero acceleration on the acceleration plot (Fig. 4C).

Muscle activity

Electromyographic patterns of S-start and C-start behaviors (Fig. 5) were consistent among trials but differed between fast-start types. MANOVA examining fast-start type and individual effects showed a significant difference across the model as a whole (Wilks' lambda, F=1.97, P<0.005). The effect of fast-start type was significant (Wilks' lambda, F=7.85, P<0.001), while the effects of individual (Wilks' lambda, F=1.40, P=0.16) and interaction between fast-start type and individual (Wilks' lambda, F=1.23, P=0.27) were not. During the S-bend of the S-start, there was nearly simultaneous EMG activity at the anterior and midbody electrode positions in the direction of rostral bending (mean relative onset times were –8.9 ms and –7.7 ms, respectively) and at the contralateral posterior electrode (mean relative onset time –6.5 ms) (Figs 5, 6; Table 3). Relative onset times for these three positions were significantly earlier (P<0.0001) than activity in the contralateral rostral and midbody electrodes and ipsilateral caudal electrode. There were also differences in the onset times of subsequent EMG activity. Following the initial bursts of EMG activity during the S-start, the ipsilateral posterior electrode fired (mean relative onset time –1.47 ms). This subsequent activity was associated with the L-bend of the tail following the initial S-bend.

During the C-start, there was nearly simultaneous muscle activity on the ipsilateral side of the body (Figs 5, 6). The mean onset times of muscle activity relative to first movement of the fish were, from anterior to posterior, –9.3 ms, –8.3 ms and –6.7 ms (Figs 5, 6; Table 3). There was no significant difference in the delay in onset times between the fast-start types.

The amplitude and duration of the initial EMG bursts were compared between the S-start and the C-start trials. Anterior ipsilateral muscle activity and midbody ipsilateral muscle activity of S- and C-starts were compared. In addition, activity was compared between the posterior contralateral electrode of the S-start and the posterior ipsilateral electrode of the C-start.

Table 3. *Electromyographic (EMG) measurements from the initial muscle activity of S-starts and C-starts by muskellunge*

	Relative onset time (ms)		Duration (ms)		Amplitude (mV)		Area (mV ms)	
Electrode position	S-start	C-start	S-start	C-start	S-start	C-start	S-start	C-start
Anterior EMG ipsilateral	–8.94±0.71	–9.25±0.55	35.95±5.88	61.26±11.50	0.69±0.12	0.90±0.14	24.08±5.58	53.27±15.40
Midbody EMG ipsilateral	–7.67±0.90	–8.32±0.75	29.95±5.70	56.63±9.72	0.61±0.13	0.44±0.06	18.15±5.31	22.57±4.32
Posterior EMG ipsilateral		–6.70±0.72		52.68±9.49		0.59±0.10		23.66±5.29
Posterior EMG contralateral	–6.52±0.79		13.95±2.56		0.56±0.15		7.71±1.67	

All measurements are means ± S.E.M.; N=15 trials per fast-start type; three trials for each of five individuals.

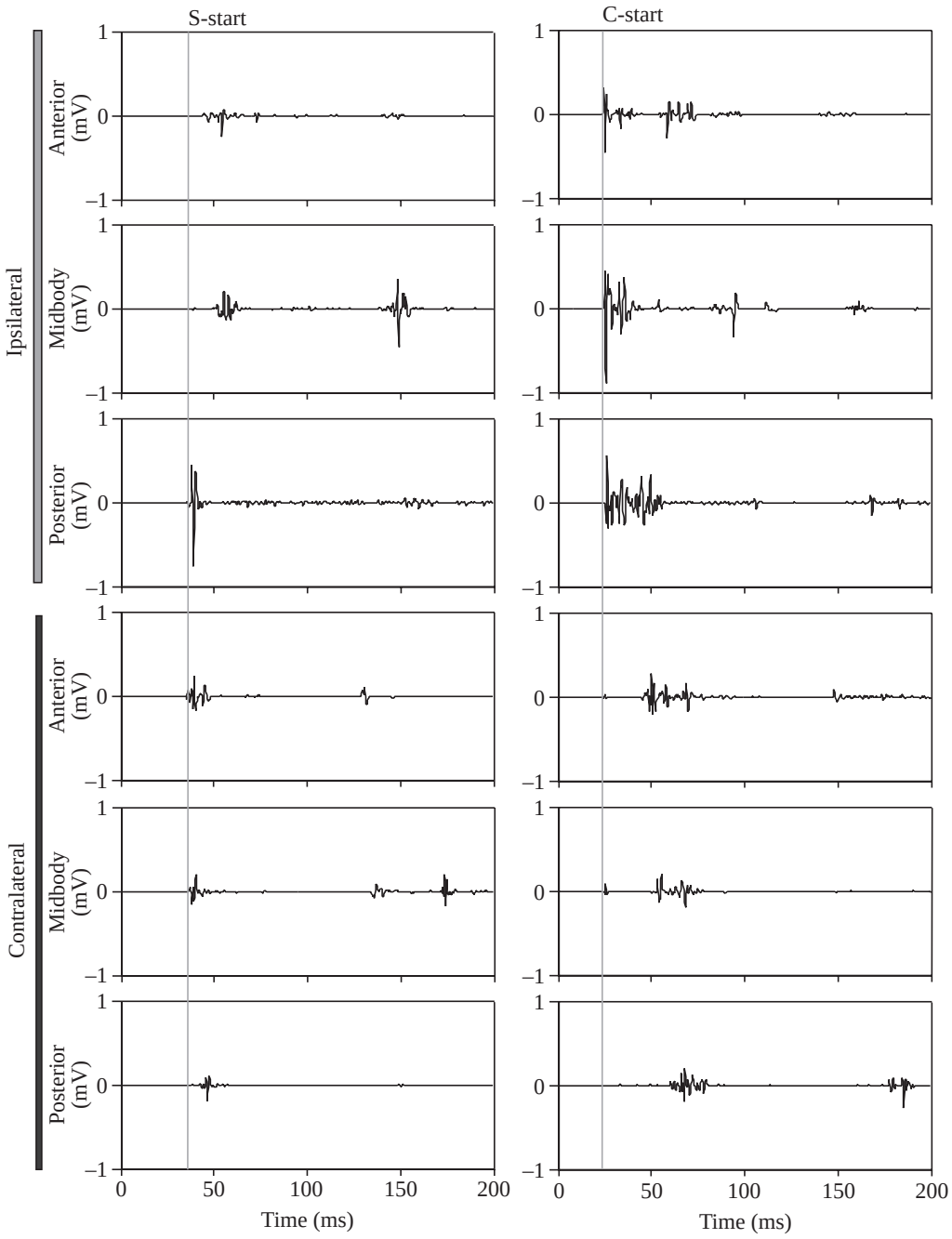

Fig. 5. Electromyographic (EMG) profiles for a typical S-start and C-start of the muskellunge. The top three panels show EMG activity on the ipsilateral side, the side of the body towards which the head moves in stage 1, and the lower three panels show contralateral EMG activity. The vertical gray lines positioned at the initiation of EMG activity provide a reference for visualizing the alignment of the activity among electrode sites.

The amplitudes of the EMG bursts did not differ significantly between the two fast-start types. Anteriorly, the duration of the initial EMG activity during the S-starts tended to be lower than that of the C-starts (anterior ipsilateral means 36 ms *versus* 61 ms; midbody ipsilateral means 30 ms *versus* 57 ms), although the difference was not significant or marginally so (P=0.0541, anterior electrode; P<0.05, midbody electrode; this was not significant after a sequential Bonferroni adjustment to significance levels; Holm, 1979; Rice, 1989). The burst duration at the posterior position was significantly shorter (P<0.0005) during the S-start than during the C-start (14 ms and 53 ms respectively).

Discussion

Testing hypotheses of S-start generation

This study tests three hypotheses for how the S-start is generated. The prevailing hypothesis has been that the S-start involves the same neural circuit as the C-start but that the body of the fish bends passively into an S shape during the response (Domenici and Blake, 1997). One alternative hypothesis is that the S-start is generated by the same neural circuit as undulatory swimming, which causes S-shaped bending waves to be formed along the body. A third hypothesis is that a neural circuit different from those generating either the C-start or undulatory swimming generates the S-start. The data for the

muskellunge presented here support the third hypothesis, that the S-start is a discrete behavior independent of the C-start or swimming and involves a neural mechanism different from those used during the C-start and swimming.

Although the S-start and C-start are both high-speed responses with comparably high angular velocity and acceleration, differences in bending patterns support the hypothesis of an alternative S-start neural circuit. Distinct bending patterns are clear when S-starts and C-starts with similar turning angles in stage 1 are compared. This can be seen by comparing the S-start depicted in Fig. 2A–F with the C-start depicted in Fig. 2G–L. In particular, bending by the tail was significantly different between the C-start and the S-start, with curvature in the same direction as anterior bending during the C-start and in the opposite direction during the S-start.

Motor pattern data also support the hypothesis that the S-start is a qualitatively different behavior from the C-start. During the C-start, there is nearly simultaneous muscle activity along one side of the body with little or no contralateral activity. This pattern of simultaneous longitudinal muscle activity has been found in numerous species (Foreman and Eaton, 1993; Jayne and Lauder, 1993; Westneat et al., 1998). In contrast, the S-start involves rostral muscle activity on one side of the body and caudal activity on the other (Figs 5, 6). Thus, during the S-start, the fish bend the caudal region of their body in the opposite direction to the rostral region to actively generate an S-shaped body curvature. The motor pattern recorded for the S-start behavior could not be generated by the neural circuit model of the C-start behavior proposed by Fetcho and Faber (1988).

In both C-start and S-start behaviors of the muskellunge, water resistance causes passive bending, as has been shown for C-starts in other taxa (Jayne and Lauder, 1996). However, this bending is largely restricted to the caudal fin (seen in Fig. 2I–J and Fig. 3D for the C-start and in Fig. 2B for the S-start). During the S-start, caudal fin flexion was in the reverse direction to the posterior bend rather than to the major anterior bend. This is the opposite direction from that to be expected if passive bending were responsible for the S-bend of the body during the S-start.

The difference between C-start and S-start kinematic patterns and the EMG data leads to the rejection of the first hypothesis for the S-start escape behavior of the muskellunge. However, there are situations in which an S-shaped behavior can result from C-start motor pattern with passive contralateral bending in the muscular part of the tail, as was shown by Jayne and Lauder (1993, 1996) for the bluegill sunfish (*Lepomis macrochirus*). It is unclear whether it will be possible to distinguish through kinematics alone an S-start generated by an S-start motor pattern and an S-shaped C-start generated by a C-start motor pattern for a given species. Additional research comparing the kinematics and EMG data for S-start and C-start may be able to describe consistent interspecific differences between these two behaviors.

It is also unlikely that the S-start is generated by the same neural circuits that are responsible for rhythmic undulatory swimming. If this were the case, the S-start would be predicted to have lower performance than the C-start. In contrast, the S-starts recorded had comparable performance with the C-starts examined, with short durations and high peak angular velocity and angular acceleration that did not differ significantly between fast-start types. The angular velocity and angular acceleration profiles for the two responses also share many characteristics of the early movements of the behavior, including similar early peaks in angular acceleration and similar deceleration at the end of the C- or S-bends.

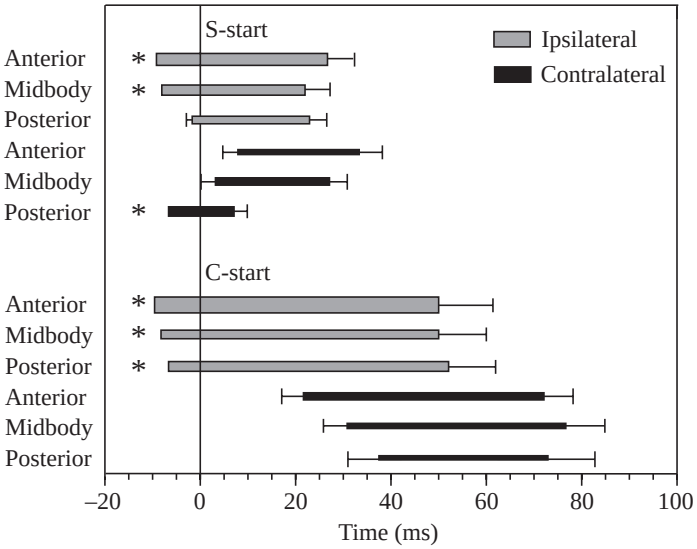

Fig. 6. Cumulative electromyographic data for S-start and C-start behaviors of the muskellunge. The lengths of the bars reflect mean duration, with standard mean error of duration shown by error bars to the right of the bars. Trials were aligned by the first kinematic movement during the responses (zero on the *x*-axis). Mean onset times relative to the first movement are indicated by the left margin of each bar, and the left-hand error bars indicate the standard error of the onset times. An asterisk indicates that the standard error of the mean was less than 1. The heights of the bars approximate the mean relative amplitude of the electromyographic activity.

Motor pattern data also imply that the S-start is not generated by the same mechanism as undulatory swimming. The neural circuits involved in rhythmic axial swimming movements cause motoneuron and muscle activity to be propagated posteriorly along the spinal cord and result in waves of muscle contraction along the body (Jayne and Lauder, 1993). A similar wave of activity would be expected during the S-start, and this was not found to be the case. Although there is a slight rostral-to-caudal delay in muscle activity onset, it is comparable with that of the C-start and can be attributed to propagation of action potentials along neurons in the spinal cord. This is considerably faster that the wave of rostral-to-caudal propagation expected during steady swimming.

These data indicate that the S-start is a fundamentally different type of startle response from the C-start in fishes. In addition to its function as an escape behavior, S-start behavior

is also used during feeding events (e.g. Hoogland et al., 1957; Webb and Skadsen, 1980; Harper and Blake, 1991). The relationship between the escape S-start and the feeding S-start is unclear. Harper and Blake (1991) showed that there was no significant difference in the performance of several classes of feeding S-starts and escape S-starts (escape data Type II and Type III for *Esox lucius* reported in Harper and Blake, 1990). Neurophysiological and muscle activity data have not been recorded from feeding S-starts, so it is not yet known whether the feeding S-start types differ in basic motor control (Domenici and Blake, 1997) or how the neural basis of the feeding S-start relates to that of the escape S-start.

Alternative neural mechanisms for generating the S-start escape response

The S-start, like the C-start, is a rapid, high-performance behavior, but it differs from the C-start in its overall patterns of muscle activity and bending. How are the motor circuits that control these two escape behaviors similar and how do they differ? Although it will be necessary to identify the neurons involved in the S-start and to examine their physiology to answer this question definitively, muscle activity patterns and comparisons with the C-start neural circuit provide important insights into how the S-start circuit may be organized. As pointed out by Eaton et al. (2001), the muscle activity patterns of the startle response provide a good indication of the startle circuit's output because the connections between reticulospinal neurons and motoneurons are simple, being either mono- or disynaptic.

The C-start is initiated by input from several reticulospinal cells, with the most prominent being the Mauthner neuron (e.g. Zottoli, 1977; Eaton et al., 1981). Mauthner neuron activity causes nearly simultaneous muscle contraction along the full length of the body on the side opposite to the stimulus. Because the S-start is a rapid, powerful response in many ways similar to the C-start, it is likely also to involve reticulospinal neurons. However, it is unlikely that the Mauthner cell functions in the S-start. EMG patterns show that, during the S-start, there is strong activity anteriorly on one side of the body and posteriorly on the opposite side. Because the Mauthner cell response is very strong, and able to override pre-existing activity in the spinal cord (Jayne and Lauder, 1993; Svoboda and Fetcho, 1996), it is unlikely that inhibitory mechanisms could allow for regional Mauthner cell activity that would generate the S-start motor pattern.

Other reticulospinal interneurons that have been shown to be involved in C-start behavior (Kimmel et al., 1980; Eaton et al., 1982; DiDomenico et al., 1988; O'Malley et al., 1996; Liu and Fetcho, 1999) and that may be active during the S-start response are the serial homologs to the Mauthner cells, MiD2 cm and MiD3 cm (Kimmel et al., 1982; Metcalfe et al., 1986; Lee and Eaton, 1991). Although activity data indicate that these cells are not involved in startle responses elicited by touching the tail in larval zebrafish (O'Malley et al., 1996), there may be interspecific differences that allow for such a function in the muskellunge. Alternatively, other reticulospinal cells not known to function during the C-start may be involved.

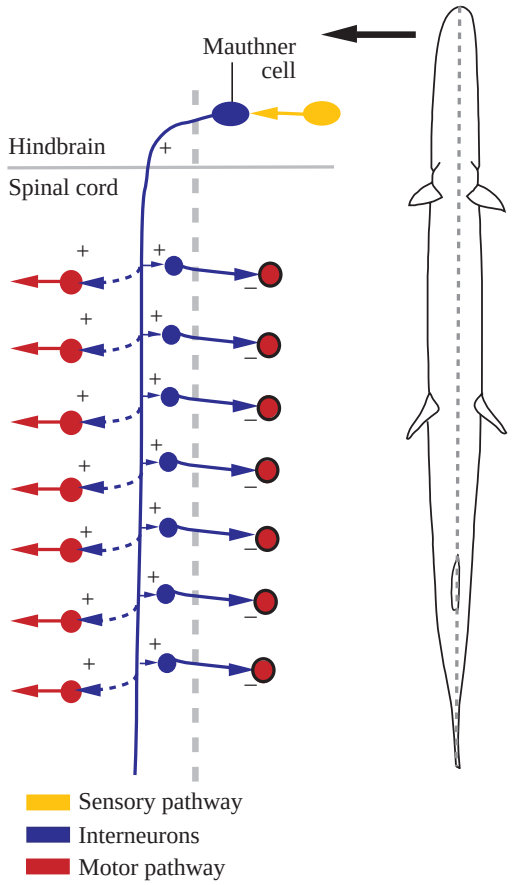

Fig. 7. A simplified diagram of the spinal cord C-start neural circuit modified from Fetcho and Faber (1988). In this diagram, the stimulus would be from the right and the fish would turn to the left. The Mauthner axon synapses with interneurons and motoneurons in the spinal cord. Directly and through excitatory interneurons (multiple known pathways indicated by a dashed line), the Mauthner cell excites motoneurons to generate the C-bend. Through commissural interneurons, it inhibits motoneuron activity on the opposite side of the body. The numbers of cells indicated in the diagram do not reflect the numbers or distributions in the fish, nor do they reflect the relative numbers of different cell types. Instead, they simply illustrate regional differences along the body.

The spinal interneurons and motoneurons involved in the C-start (Fetcho and Faber, 1988) are likely also to function in the S-start because their roles in the two startle response types would be similar: fast, powerful activation of lateral muscle. During the C-start, excitatory interneurons and motoneurons are active along the full length of the body on one side and are inhibited through commissural inhibitory interneurons on the other (Fetcho and Faber, 1988). During the S-start, these circuits would have to be active on one side of the spinal cord anteriorly and on the opposite side posteriorly.

On the basis of the muscle activity patterns of the S-start and the C-start and on models for the C-start neural circuit, I suggest two general models for how the S-start is generated

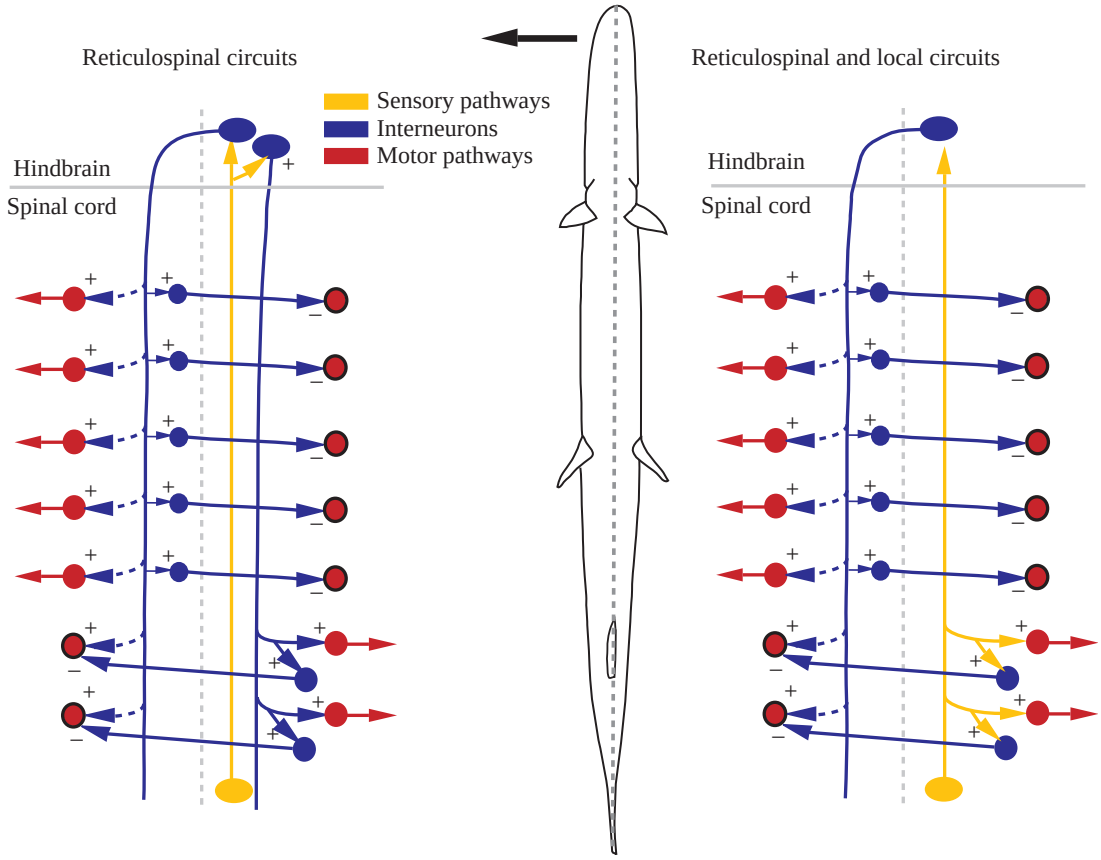

Fig. 8. Alternative neural circuit models for the S-start startle response. The left-hand circuit depicts a possible S-start mechanisms involving multiple reticulospinal pathways. Commissural and ipsilateral reticulospinal cells cause motoneuron and muscle activity regionally in the spinal cord. The right-hand circuit depicts a possible C-start model involving a combination of reticulospinal and local circuits. Anterior activity is determined through descending reticulospinal commands, while posterior activity is generated through local spinal cord circuits. The spinal cord interneurons are presumed to be the same as those used in the C-start and are depicted as such. The numbers of cells indicated in the diagrams do not reflect the numbers or distributions in the fish, nor do they reflect the relative numbers of different cell types. Instead, they simply illustrate regional differences along the body

neurally. The first involves a combination of reticulospinal cells that have their output restricted to different regions of the spinal cord. In the second, the S-start is activated by a combination of reticulospinal and local input to spinal cord.

Fig. 7 shows the neural circuit of the C-start based on pairwise intracellular recordings (Fetcho and Faber, 1988). A stimulus from the same side of the body as the Mauthner cell soma causes the cell to fire an action potential. That action potential travels down the axon, crossing the midline of the body to excite interneurons and motoneurons on the opposite side of the body from the Mauthner cell soma. Both directly and indirectly through excitatory interneurons, the Mauthner cell excites motoneurons to fire and the lateral muscle to contract.

The first model for the S-start (Fig. 8 left), like the C-start, involves spinal interneuron and motoneurons driven by the activity of several reticulospinal neurons or groups of reticulospinal neurons in the hindbrain. A stimulus to the tail causes ascending sensory neurons to excite reticulospinal interneurons that descend on both sides of the spinal cord to activate the trunk and tail motoneurons and musculature regionally. An example of this scenario (Fig. 8 left) shows one set of reticulospinal interneurons exciting spinal circuits posteriorly to cause muscle contraction on the same side of the body and inhibit it on the opposite side. Another set of reticulospinal interneurons crosses the spinal cord and descends to excite rostral muscle to contract on the opposite side of the body. Similarly, commissural inhibitory interneurons prevent bilateral activity anteriorly.

A second model for the S-start neural circuit differs from the C-start circuit in that it involves a combination of reticulospinal interneurons and local circuits. An example of this type of circuit (Fig. 8 right) involves a caudal stimulus that excites spinal circuits directly in the tail in addition to ascending to the hindbrain to trigger reticulospinal cells. The caudal circuits cause muscle activity on one side of the body and inhibit contralateral activity posteriorly. The axons of the reticulospinal interneurons descend into the spinal cord, exciting interneurons and motoneurons on the opposite side to the body from the caudal excitation. Commissural inhibitory interneurons, as in the other models, prevent conflicting bilateral activity.

The proposed circuit diagrams (Fig. 8) provide examples of two basic models of the S-start. Many other configurations are possible for each general model, reticulospinal or reticulospinal together with local control, that could generate the same muscle activity patterns. Optical imaging techniques for examining physiology (O'Malley et al., 1996; Liu and Fetcho, 1999) and morphology (Hale et al., 2001) provide powerful approaches for examining the S-start neural circuit in greater detail. The S-start behavior and its motor control mechanisms provide a comparative model to the C-start neural circuit to give a basic understanding of startle behaviors and neural circuit organization.

Most of this work was performed while I was a postdoctoral fellow in the Department of Neurobiology and Behavior at the State University of New York at Stony Brook. I wish to thank Joe Fetcho for discussions about startle behavior neurobiology, Mark Westneat for the use of equipment and assistance and Steve Krueger for supplying the fish used in these experiments. Thanks also to Joe Fetcho, John Long, Jeff Walker, Mark Westneat and two anonymous reviewers for their comments on this manuscript. This work was funded by National Institute of Health NRSA MH11861.

References

DiDomenico, R., Nissanov, J. and Eaton, R. C. (1988). Lateralization and adaptation of a continuously variable behavior following lesions of a reticulospinal command neuron. *Brain Res.* **473**, 15–28.

Domenici, P. and Blake, R. W. (1991). The kinematics and performance of the escape response in the angelfish (*Pterophyllum eimekei*). *J. Exp. Biol.* **156**, 187–205.

Domenici, P. and Blake, R. W. (1997). The kinematics and performance of fish fast-start swimming. *J. Exp. Biol.* **200**, 1165–1178.

Eaton, R. C., Lavender, W. A. and Weiland, C. M. (1981). Identification of the Mauthner initiated response patterns in goldfish: evidence from simultaneous cinematography and electrophysiology. *J. Comp. Physiol. A* **144**, 521–531.

Eaton, R. C., Lavender, W. A. and Weiland, C. M. (1982). Alternative neural pathways initiate fast-start responses following lesions of the Mauthner neuron in goldfish. *J. Comp. Physiol. A* **145**, 485–496.

Eaton, R. C., Lee, R. K. K. and Foreman, M. B. (2001). The Mauthner cell and other identified neurons of the brainstem escape network of fish. *Prog. Neurobiol.* **63**, 467–485.

Faber, D. S., Fetcho, J. R. and Korn, H. (1989). Neuronal networks underlying the escape response in goldfish: general implications for motor control. *Ann. N.Y. Acad. Sci*. **563**, 11–33.

Fetcho, J. R. (1990). Morphological variability, segmental relationships and a functional role of a class of commissural interneurons in the spinal cord of goldfish. *J. Comp. Neurol.* **299**, 283–298.

Fetcho, J. R. (1991). The spinal network of the Mauthner cell. *Brain Behav. Evol.* **37**, 298–316.

Fetcho, J. R. and Faber, D. S. (1988). Identification of motoneurons and interneurons in the spinal network for escapes initiated by the Mauthner cell in goldfish. *J. Neurosci.* **8**, 4192–4213.

Foreman, M. B. and Eaton, R. C. (1993). The direction change concept for reticulospinal control of goldfish escape. *J. Neurosci.* **13**, 4101–4133.

Frith, H. R. and Blake, R. W. (1995). The mechanical power output and the hydromechanical efficiency of northern pike (*Esox lucius*) fast-starts. *J. Exp. Biol.* **198**, 1863–1873.

Furukawa, T. and Furshpan, E. J. (1963). Two inhibitory mechanisms in the Mauthner neurons of goldfish. *J. Neurophysiol.* **26**, 140–176.

Hackett, J. T. and Faber, D. S. (1983). Relay neurons mediate collateral inhibition of the goldfish Mauthner cell. *Brain Res.* **264**, 302–306.

Hale, M. E., Ritter, D. A. and Fetcho, J. R. (2001). A confocal study of spinal interneurons in living larval zebrafish. *J. Comp. Neurol.* **437**, 1–16.

Harper, D. G. and Blake, R. W. (1990). Fast-start performance of rainbow trout *Salmo gairdneri* and northern pike *Esox lucius*. *J. Exp. Biol.* **150**, 321–342.

Harper, D. G. and Blake, R. W. (1991). Prey capture and the fast-start performance of northern pike *Esox lucius*. *J. Exp. Biol.* **155**, 175–192.

Holm, S. (1979). A simple sequentially rejective multiple test procedure. *Scand. J. Stat.* **6**, 65–70.

Hoogland, R., Morris, D. and Tinbergen, N. (1957). The spines of the stickleback as a means of defense against predators (*Perca* and *Esox*). *Behaviour* **10**, 88–104.

Jayne, B. C. and Lauder, G. V. (1993). Red and white muscle activity and kinematics of the escape response of bluegill sunfish during swimming. *J. Comp. Physiol. A* **173**, 495–508.

Jayne, B. C. and Lauder, G. V. (1995). Speed effects on midline kinematics during steady undulatory swimming of largemouth bass, *Micropterus salmoides*. *J. Exp. Biol.* **198**, 585–602.

Jayne, B. C. and Lauder, G. V. (1996). New data on axial locomotion in fishes: How speed affects diversity of kinematics and motor patterns. *Am. Zool.* **36**, 642–655.

Johnston, I. A., Van Leeuwen, J. L., Davies, M. L. F. and Bedow, T. (1995). How fish power predation fast-starts. *J. Exp. Biol.* **198**, 1851–1861.

Kimmel, C. B., Eaton, R. C. and Powell, S. L. (1980). Decreased fast-start performance of zebrafish larvae lacking Mauthner neurons. *J. Comp. Physiol.* **140**, 343–350.

Kimmel, C. B., Powell, S. L. and Metcalfe, W. K. (1982). Brain neurons which project to the spinal cord in young larvae of the zebrafish. *J. Comp. Neurol.* **205**, 112–127.

Lee, R. K. K. and Eaton, R. C. (1991). Identifiable reticulospinal neurons of the adult zebrafish, *Brachydanio rerio*. *J. Comp. Neurol.* **304**, 34–52.

Liu, K. S. and Fetcho, J. R. (1999). Laser ablations reveal functional relationships of segmental hindbrain neurons in zebrafish. *Neuron* **23**, 325–335.

Metcalfe, W. K., Mendelson, B. and Kimmel, C. B. (1986). Segmental homologies among reticulospinal neurons in the hindbrain of the zebrafish larva. *J. Comp. Neurol.* **251**, 147–159.

O'Malley, D. M., Kao, Y.-H. and Fetcho, J. R. (1996). Imaging the functional organization of zebrafish hindbrain segments during escape behaviors. *Neuron* **17**, 1145–1155.

Rand, D. M. and Lauder, G. V. (1981). Prey capture in the chain pickerel, *Esox niger*: correlations between feeding and locomotor behaviour. *Can J. Zool.* **59**, 1072–1078.

Rice, W. R. (1989). Analyzing tables of statistical tests. *Evolution* **43**, 223–225.

Spierts, I. L. and Van Leeuwen, J. L. (1999). Kinematics and muscle dynamics of C- and S-starts of carp (*Cyprinus carpio* L.). *J. Exp. Biol.* **202**, 393–406.

Svoboda, K. R. and Fetcho, J. R. (1996). Interaction between the neural networks for escape and swimming in goldfish. *J. Neurophysiol.* **16**, 843–852.

Walker, J. A. (1998). Estimating velocities and accelerations of animal locomotion: a simulation experiment comparing numerical differentiation algorithms. *J. Exp. Biol.* **74**, 211–266.

Webb, P. W. (1976). The effect of size on the fast-start performance of rainbow trout (*Salmo gairdneri*). *J. Exp. Biol.* **65**, 157–177.

Webb, P. W., Hardy, D. H. and Mehl, V. L. (1992). The effect of armored skin on the swimming of longnose gar, *Lepisosteus osseus*. *Can. J. Zool.* **70**, 1173–1179.

Webb, P. W. and Skadsen, J. M. (1980). Strike attacks of *Esox*. *Can. J. Zool.* **58**, 1462–1469.

Weihs, D. (1973). The mechanism of rapid starting of slender fish. *Biorheology* **10**, 343–350.

Westneat, M. W., Hale, M. E., McHenry, M. J. and Long, J. H. (1998). Mechanics of the fast-start: muscle function and the role of intramuscular pressure in the escape behavior of *Amia calva* and *Polypterus palmas*. *J. Exp. Biol.* **201**, 3041–3055.

Zottoli, S. J. (1977). Correlation of the startle reflex and Mauthner cell auditory responses in unrestrained goldfish. *J. Exp. Biol.* **66**, 65–81.